Chinese Chemical Letters 36 (2025) 110008

Contents lists available at ScienceDirect

Chinese Chemical Letters

journal homepage: www.elsevier.com/locate/cclet

High-performance room temperature solid-state lithium battery enabled by PP-PVDF multilayer composite electrolyte

Sheng Zhao[1], Junjie Lu[1], Bifu Sheng, Siying Zhang, Hao Li, Jizhang Chen, Xiang Han*

College of Materials Science and Engineering, Co-Innovation Center of Efficient Processing and Utilization of Forest Resources Nanjing Forestry University, Nanjing 210037, China

ARTICLE INFO

Article history:
Received 24 March 2024
Revised 24 April 2024
Accepted 13 May 2024
Available online 14 May 2024

Keywords:
Lithium-ion batteries
Composite solid electrolyte
Interface stability
Mechanical properties
Room temperature cycling

ABSTRACT

Solid-state batteries (SSBs) with thermal stable solid-state electrolytes (SSEs) show intrinsic capacity and great potential in energy density improvement. SSEs play critical role, however, their low ionic conductivity at room temperature and high brittleness hinder their further development. In this paper, polypropylene (PP)-polyvinylidene fluoride (PVDF)-$Li_{1.3}Al_{0.3}Ti_{1.7}(PO_4)_3$ (LATP)-Lithium bis(trifluoromethane sulphonyl)imide (LiTFSI) multi-layered composite solid electrolyte (CSE) is prepared by a simple separator coating strategy. The incorporation of LATP nanoparticle fillers and high concentration LiTFSI not only reduces the crystallinity of PVDF, but also forms a solvation structure, which contributes to high ionic conductivity in a wide temperature. In addition, using a PP separator as the supporting film, the mechanical strength of the electrolyte was improved and the growth of lithium dendrites are effectively inhibited. The results show that the CSE prepared in this paper has a high ionic conductivity of 6.38×10^{-4} S/cm at room temperature and significantly improves the mechanical properties, the tensile strength reaches 11.02 MPa. The cycle time of Li/Li symmetric cell assembled by CSE at room temperature can exceed 800 h. The Li/LFP full cell can cycle over 800 cycles and the specific capacity of Li/LFP full cell can still reach 120 mAh/g after 800 cycles at 2 C. This CSE has good cycle stability and excellent mechanical strength at room temperature, which provides an effective method to improve the performance of solid electrolytes under moderate condition.

With the wide application of lithium-ion batteries (LIBs) on new energy electric vehicles (EVs), their energy density and safety is receiving increasing attention [1,2]. Electrolyte, as a key component in lithium-ion batteries, plays a role in conducting ions between the positive and negative electrodes [3]. It needs to have a series of advantages such as good electrochemical stability, high ionic conductivity, high thermal stability and a wide temperature range for operation [4]. It is a guarantee for lithium-ion batteries to obtain high voltage, high specific energy, and other advantages. Traditional liquid electrolytes are prone to side reactions with lithium metals, which cannot effectively inhibit the growth of lithium dendrites, leading to short circuits and thermal runaway in batteries [5-7]. By contrast, solid-state electrolytes (SSEs) have excellent mechanical properties, and electrochemical stability, and can inhibit dendrite growth, making them the core material for preparing all solid-state lithium batteries with higher safety [8-10].

Compared to inorganic SSEs, polymer SSEs exhibit good flexibility and stable interfaces, which has attracted much attention [11-13]. Specifically, due to its excellent flexibility, thermal stability, and electrochemical stability, PVDF has become one of the most attractive polymer electrolytes [14]. However, under room temperature conditions, the poor ionic conductivity of PVDF electrolyte seriously affect its practical application [15]. Many scholars have proposed that metal-organic frameworks (MOFs) can accelerate the migration of lithium ions in PVDF-based solid electrolytes [16], as MOFs themselves can act as ion conductors and provide additional transport channels for lithium ions [17]. However, due to their porous structure, they cannot form a dense solid electrolyte with PVDF, resulting in uneven ion conductivity and unstable interface with the electrode. Therefore, designing and preparing dense PVDF-based electrolytes with excellent ionic conductivity still faces significant challenges.

Furthermore, the mixing of inorganic ceramic electrolytes and polymer electrolytes can reduce the crystallinity of polymers and improve the properties of polymer-based electrolytes [18,19]. NASICON type ceramic $Li_{1.5}Al_{0.5}Ti_{1.5}(PO_4)_3$ (LATP) exhibits high ion conductivity (10^{-4}–10^{-3} S/cm) and optimal air stability at room tem-

* Corresponding author.
E-mail address: hanxiang@njfu.edu.cn (X. Han).
[1] These authors contributed equally to this work.

https://doi.org/10.1016/j.cclet.2024.110008
1001-8417/

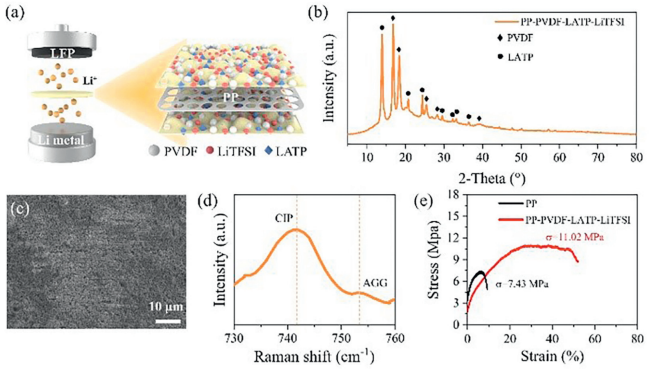

Fig. 1. (a) Schematic diagram of battery prepared with PP-PVDF-LATP-LiTFSI multi-layered CSE. (b) XRD pattern of PP-PVDF-LATP-LiTFSI multi-layered CSE. (c) Surface SEM image of PP-PVDF-LATP-LiTFSI multi-layered CSE. (d) Raman spectra of PP-PVDF-LATP-LiTFSI multi-layered CSE. (e) Stress-strain curves of PP separator and PP-PVDF-LATP-LiTFSI multi-layered CSE.

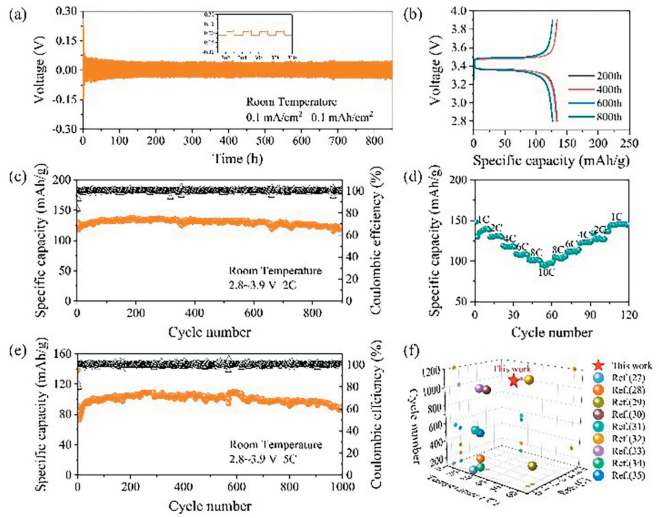

Fig. 2. (a) Charge/discharge curve of Li/Li symmetric cell with PP-PVDF-LATP-LiTFSI multi-layered CSE at the current density of 0.1 mA/cm^2. (b) The charge and discharge voltage platform of Li/LFP full cell with PP-PVDF-LATP-LiTFSI multi-layered CSE during the cycle at 2 C. Long-term cycling performance of Li/LFP full cell with PP-PVDF-LATP-LiTFSI multi-layered CSE at (c) 2 C and (e) 5 C. (d) Rate performance of Li/LFP full cell with PP-PVDF-LATP-LiTFSI multi-layered CSE. (f) Performance comparison of Li/LFP cells with different solid electrolytes in rencent articles [27-35].

perature [20], which can improve the physical and chemical properties of SPEs while providing more effective lithium ion channels. However, it has problems such as high brittleness and high interfacial impedance between electrodes. Moreover, in many studies of composite solid electrolytes (CSEs) based on PVDF-LATP, the cycling at room temperature is unstable and the mechanical properties are poor. Therefore, it is crucial to prepare a solid-state PVDF-based electrolyte that achieves stable cycling at room temperature.

Therefore, we use a simple separator coating strategy to prepare PP-PVDF-LATP-LiTFSI multi-layered CSEs, to improve the various properties of the electrolyte. Compared to liquid electrolytes, the CSEs we prepared in this study can effectively reduce the occurrence of side reactions, making it safer and more stable. Secondly, mixing LATP as nanoparticle fillers with PVDF helps to prevent the ordered aggregation of polymer chains, reduce the crystallinity of PVDF, increase the amorphous region, and facilitate Li^+ migration [21]. In addition the mass ratio of LiTFSI to PVDF polymer, which may increase the ratios of AGGs and CIPS in the solvation shell, thereby improving the overall ion conductivity, and facilitating the formation of dense solid-solid contact with electrode active materials, and maintaining contact for a long time during the electrochemical cycling process. Coupled with PP separator as the supporting film as support, it increases the mechanical strength of the electrolyte, effectively inhibits lithium dendrite growth, and improves the energy density and cycling capacity retention rate of the battery. It is worth mentioning that the CSEs prepared in this study expand the temperature range of battery use, and can maintain good cycling stability even at room temperature. The research on this topic is expected to improve the performance of solid-state electrolytes and provide assistance for the application of all-solid-state lithium batteries.

In this paper, CSEs were prepared by a simple separator coating method (Fig. 1a). The CSE was based on PP separator and coated with PVDF-LATP-LiTFSI coating on both sides. Its thickness is 55 μm. Theoretically, the CSE prepared in this study can improve the mechanical properties and increase the toughness of the solid electrolyte, on the other hand, it can effectively improve the electrochemical performance and achieve stable circulation at room temperature. The X-ray diffraction (XRD) pattern is shown in Fig. 1b. The characteristic peaks of PVDF and LATP are obvious, indicating that PVDF and LATP are well mixed, and the peak of LiTFSI disappears in the XRD pattern, indicating that the PVDF-LATP system has excellent Li salt solubility [22]. From the scanning electron microscope (SEM) shown in Fig. 1c, it can be seen that the particle size on the surface of the PP separator is uniform without agglomeration. LATP particles are evenly distributed on the surface and internal pores of PVDF, reducing the size of pore defects and forming dense CSE, which is in line with the expected assumption and can effectively inhibit the growth of lithium dendrites [23]. The Raman spectra (Fig. 1d) showed CIP (contact ion pair) and AGG (small aggregate) near 741 cm^{-1} and 753 cm^{-1}, respectively, indicating that Li^+ and $TFSI^-$ gathered to form ion clusters, which improved the ionic conductivity of solid electrolyte, thereby inhibiting the growth of lithium dendrites, reducing the interface impedance, and improving the electrochemical performance of the battery [24]. The better the mechanical properties of solid electrolyte, the better the inhibition effect on lithium dendrite growth, and the stronger the ability to resist lithium dendrite puncture [19]. In order to analyze the mechanical properties of CSE, we conducted tensile tests on PP-PVDF-LATP-LiTFSI multi-layered CSE and PP separator (Fig. 1e). The results showed that the tensile strength of CSE was 11.02 MPa, significantly higher than that of the PP separator, The results show that PVDF-LATP-LiTFSI multi-layered will not reduce the mechanical strength of the PP separator. The tensile strength of pure PVDF solid electrolyte studied in the past is about 4.5 MPa, which is far lower than that of this CSE. This is because with PP as the supporting film, PVDF-LATP is evenly distributed in the CSE as a skeleton structure, which improves the mechanical property of CSE. In addition, due to the good flexibility of PVDF, the mechanical strength of CSE is improved while it still has good flexibility, so that the interface between CSE and electrode is in good contact, which is conducive to the stability of the interface.

In order to verify the cycle stability of CSE, we assembled Li/Li symmetric cell and Li/LFP full cell, and conducted charge discharge cycles on them. The Li/Li symmetric cell was charged and discharged at room temperature with current density of 0.1 mA/cm^2 and 0.25 mA/cm^2 respectively. Fig. 2a shows that the Li/Li symmetric cell assembled with PP-PVDF-LATP-LiTFSI multi-layered CSE can cycle stably for more than 800 h at current density of 0.1 mA/cm^2 and for more than 200 h at current density of 0.25 mA/cm^2 (Fig. S1 in Supporting information). Further, from partial enlarged drawing, it can be found that its overpotential is stable at 30 mA and 50 mA respectively, indicating that the CSE prepared in this study can increase the stability of the interface between the electrode and electrolyte. It can inhibit the growth of lithium dendrite and prolong the life of the battery. Moreover, We conducted critical current density test on Li/Li symmetric cell, and the result is shown in

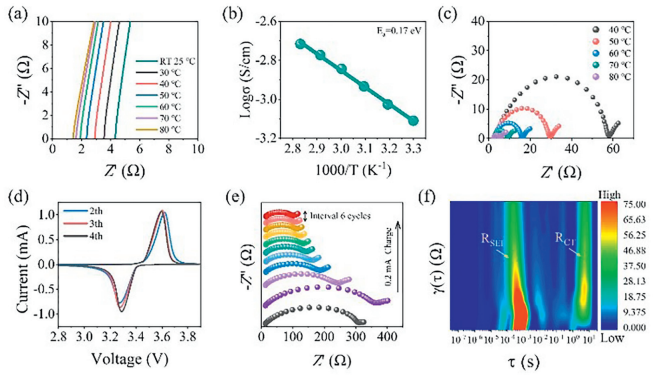

Fig. 3. (a) AC impedance spectra of stainless steel symmetric cells at different temperatures. (b) Arrhenius curve of stainless steel symmetric cells with PP-PVDF-LATP-LiTFSI multi-layered CSE. (c) EIS patterns of Li/Li symmetric cells. (d) The CV curve of Li/LFP full cell during the 2–4 cycling. (e) *In situ* impedance of Li/Li symmetric cell. (f) EIS-DRT measurement of Li/Li symmetric cell.

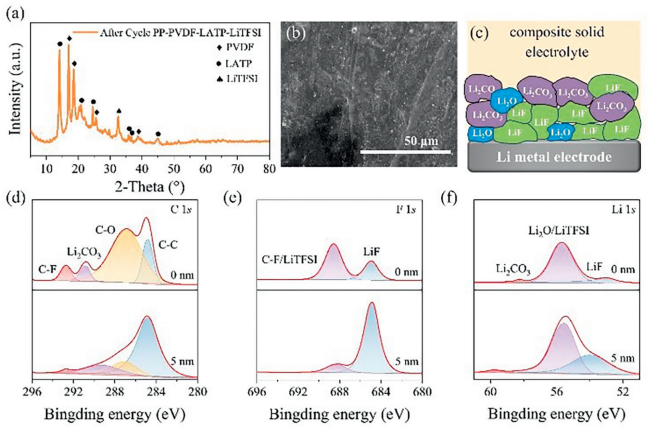

Fig. 4. (a) XRD pattern of PP-PVDF-LATP-LiTFSI multi-layered CSE after cycling. (b) Surface SEM image of lithium metal sheet after 1000 cycles. (c) Schematic diagram of surface/interface between CSE and lithium metal. (d) C 1s, (e) F 1s and (f) Li 1s spectra of composite solid electrolyte and lithium surface/interface under different etching degrees.

Fig. S2 (Supporting information). Li/Li symmetric cell can achieve a critical current density of 3.75 mA/cm^2, indicating its high ability for suppressing Li dendrites during repeated cycling. Similarly, the Li/LFP full cell was assembled with PP-PVDF-LATP-LiTFSI multi-layered CSE at room temperature and the cycle test was carried out. We were surprised to find that the specific capacity of the battery we assembled could reach 130 mAh/g at 2 C (1 C = 140 mAh/g) (Fig. 2c), and the coulomb efficiency remained stable at about 100%. Specifically, Fig. 2b shows the relationship between voltage and specific capacity at 200, 400, 600 and 800 cycles. The curve coincidence degree is good, and the charging and discharging platform is relatively stable, indicating that the battery cycle is stable. Similarly, as shown in Fig. 2e, the specific discharge capacity of the cell at 5 C is maintained at about 110 mAh/g, and the coulomb efficiency is still maintained at about 100%. After 1000 cycles, the capacity retention rate is 80% (Fig. S3 in Supporting information). On the one hand, the prepared CSE can form a dense solid-solid contact with the electrode, effectively reduce side reactions, inhibit the growth of lithium dendrites, and improve the cycle stability. On the other hand, the high concentration of LiTFSI provides a large amount of free Li^+ and $TFSI^-$ and also aggregates to form ion clusters, forming a unique fast conduction channel through the connection of filler LATP [25]. In order to study the rate performance of the full battery, the PP-PVDF-LATP-LiTFSI multi-layered CSE was used to assemble the Li/LFP full cell to charge/discharge at the rate of 1, 2, 4, 6, 8 and 10 C at room temperature (Fig. 2d), gradually increasing from 1 C to 10 C, and then returning to 1 C. The discharge specific capacities were 140, 131, 118, 108, 100 and 97 mAh/g respectively (Fig. S4 in Supporting information). It is not difficult to find that the specific capacity of the cell can be maintained at 97 mAh/g even at the high rate of 10 C. When the current density falls back to 1 C, the capacity can return to the original state, which is due to the high ionic conductivity of CSE and the fast migration path of lithium ions [26]. It also shows that the stable interface between CSE and electrode can greatly reduce the polarization of the battery. Compared with the solid electrolytes in other recent articles, the CSE in this paper has excellent performance in terms of temperature, cycle number and magnification, and can achieve stable and long cycle at room temperature (Fig. 2f) [27-35].

In order to further study the electrochemical performance of CSE, we prepared stainless steel|PP-PVDF-LATP-LiTFSI|stainless steel cell and Li|PP-PVDF-LATP-LiTFSI|Li cell, and conducted EIS test on them at different temperatures (Figs. 3a and c). Calculate the lithium-ion conductivity according to Eq. S1 (Supporting information). The Arrhenius diagram of CSE is obtained by lithium-ion conductivity, as shown in Fig. 3b and Fig. S5 (Supporting information). It can be found that CSE has excellent ionic conductivity in both stainless steel symmetric cells and Li/Li symmetric cells. The ionic conductivity of pure PVDF electrolyte is only 3.6×10^{-5} S/cm [26]. However, the ionic conductivity of CSE can reach 6.38×10^{-4} S/cm even at room temperature (see Table S2 in Supporting information for comparison with ionic conductivity of solid eelectrolytes in other articles). Moreover, its electronic conductivity is 1.375×10^{-10} S/cm (Fig. S6 in Supporting information). The difference between ionic conductivity and electronic conductivity is 6 orders of magnitude, indicating that CSE can improve the migration rate of lithium ions and effectively inhibit the growth of lithium dendrites [36]. The activation energy is 0.17 eV in the stainless steel symmetric cell and 0.39 eV in the Li/Li symmetric cell, indicating that the CSE prepared in this study has a dense surface, which effectively improves the porous characteristics of PVDF electrolyte [26]. It is conducive to the stable circulation of the battery at room temperature. We also tested Li/LFP full cell by cyclic voltammetry (CV). As shown in Fig. 3d, in the process of battery charging and discharging, there are only peaks around 3.3 V and 3.6 V, which are the characteristic peaks of lithium iron phosphate [37], indicating that the battery has no obvious side reactions and has good stability. This means that the prepared CSE does not participate in the electrochemical reaction process, but only provides a channel for lithium ion migration. In order to test the interface stability of Li/Li symmetric cells during cycling, *in-situ* impedance measurements were carried out. Fig. S7 (Supporting information) reveals the voltage change during the cycle, which is consistent with the fitted Arrhenius diagram (Fig. 3e). In the first 2 h, the impedance of the battery firstly increases, and then gradually decreases to stable, which is the same as the result of the charge-discharge cycle. This process is the film-forming process of SEI film. The thermal diagram is drawn through DRT analysis. As shown in Fig. 3f, it can be clearly seen that the grain boundary impedance is concentrated in about 10^{-3} s, corresponding to the semicircle of the Arrhenius diagram. This process is closely related to lithium ion migration [38], while the low-frequency diffusion process is mainly in 7 s.

The structure and surface composition of metal lithium sheet and PP-PVDF-LATP-LiTFSI multi-layered CSE after 1000 cycles were studied to further evaluate the stability of the electrode sheet and CSE. Fig. 4a XRD spectrum shows that there is no detected difference in the overall structure between the original CSE and the recycled CSE, and only the peak at 32° becomes stronger. This peak

is LiTFSI [39], indicating that CSE has no significant side reaction with the electrode during the cycle, and the interface stability is good, and the lithium-rich coordination compound [Li(DMF)$_n$TFSI] was formed and it can improve the ionic conductivity [25]. Fig. 4b shows the surface morphology of the lithium metal sheet after 1000 cycles. It can be observed that the surface of the lithium metal sheet is relatively flat without sharp dendrites, indicating that CSE can better induce uniform deposition of Li^+ and inhibit the formation of Li dendrites [40]. The X-ray photoelectron spectroscopy (XPS) results of CSE show that the C 1s spectrum includes C−C (284.8 eV), C−O (286.82 eV), Li_2CO_3 (290.81 eV) and C−F (292.74 eV) (Fig. 4d), which are derived from the decomposition fragments of PVDF polymer [41]. The F 1s spectrum (Fig. 4e) can be divided into two peaks of 684.57 eV and 684.95 eV, corresponding to LiF and C−F/LiTFSI species, respectively. In the Li 1s spectrum (Fig. 4f), there are signal peaks of 52.98 eV, 55.68 eV and 58.24 eV, corresponding to LiF, LiO_2/LiTFSI and Li_2CO_3, respectively. The appearance of LiF is mainly due to the decomposition of LiTFSI [42]. Previous studies have shown that although the ionic conductivity of LiF is not high, as an artificial SEI, it cannot only improve the stability of solid electrolyte to lithium anode, but also maintain the rapid transmission of lithium ions [43]. Fig. 4c shows that with the increase of etching degree, the Li_2CO_3 content decreases and LIF content increases at the interface between CSE and lithium metal, which indicates that CSE can improve the cycle stability of the battery, because Li_2CO_3 as a wide gap insulator will lead to a higher charging platform, resulting in a large amount of side reactions [44]. The addition of LiF can homogenize the Li^+ flux and inhibit the growth of lithium crystals [45]. It is obvious that the CSE prepared in this study has good stability at the interface with lithium metal, which effectively inhibits the growth of lithium dendrites.

In conclusion, the CSE prepared in this paper has high ionic conductivity and good mechanical properties at room temperature, and then achieve stable cycle and excellent rate performance. LATP as fillers with high ionic conductivity are evenly distributed on the surface and internal pores of PVDF to reduce the size of pore defects. In addition, a large number of free Li^+ and $TFSI^-$ provided by high concentration of LiTFSI are aggregated to form ion clusters. Through the connection of LATP fillers, a unique fast conduction channel is formed, which can not only improve the overall ionic conductivity but also effectively inhibit the growth of lithium dendrites, and then realizing the stable cycle of lithium-ion battery at room temperature. The Li/Li symmetric cell assembled by CSE at room temperature can cycle stably for more than 1000 cycles at a current density of 0.1 mA/cm^2, and the Li/LFP full cell can cycle for more than 800 cycles at 2 C. What is more, PVDF is a polymer with good toughness. With PP separator as the supporting film, it not only ensures the mechanical strength of CSE, but also has good toughness. The SEM images of the lithium metal sheet after cycling confirmed that the CSE was not easy to be pierced by lithium dendrites, which inhibited the growth of lithium dendrites to a certain extent. According to the XRD and XPS spectra after cycling, we can also find that the CSE has no obvious side reaction with lithium anode, and the interface stability is good. This study provides enlightenment for the design of CSE which can achieve stable cycling of lithium-ion batteries at room temperature.

Declaration of competing interest

The authors declare that they have no known competing financial interests or personal relationships that could have appeared to influence the work reported in this paper.

CRediT authorship contribution statement

Sheng Zhao: Writing – original draft, Validation. **Junjie Lu:** Methodology, Formal analysis. **Bifu Sheng:** Conceptualization. **Siying Zhang:** Software, Investigation. **Hao Li:** Software, Resources. **Jizhang Chen:** Project administration, Data curation, Conceptualization. **Xiang Han:** Writing – review & editing, Funding acquisition.

Acknowledgment

The work was finiancially supported by National Natural Science Foundation of China (No. 22209075).

Supplementary materials

Supplementary material associated with this article can be found, in the online version, at doi:10.1016/j.cclet.2024.110008.

References

[1] F.M.N.U. Khan, M.G. Rasul, A.S.M. Sayem, N. Mandal, Energy Rep. 9 (2023) 11–21.
[2] S. Zhao, Z. Guo, K. Yan, et al., Energy Storage Mater. 34 (2021) 716–734.
[3] B. Li, P. Wang, B. Xi, et al., Nano Res. 15 (2022) 8972–8982.
[4] P. Prakash, B. Fall, J. Aguirre, et al., Nat. Mater. 22 (2023) 627–635.
[5] Q. Wu, M. Fang, S. Jiao, et al., Nat. Commun. 14 (2023) 6296.
[6] Y. Xiang, M. Tao, X. Chen, et al., Nat. Commun. 14 (2023) 177.
[7] X. Cao, X. Ren, L. Zou, et al., Nat. Energy 4 (2019) 796–805.
[8] X. Han, S. Wang, Y. Xu, et al., Energy Environ. Sci. 14 (2021) 5044–5056.
[9] J. Kang, N. Deng, B. Cheng, et al., J. Energy Chem. 92 (2024) 26–42.
[10] M.J. Lee, J. Han, K. Lee, et al., Nature 601 (2022) 217–222.
[11] C. Xue, S. Guan, B. Hu, et al., Energy Storage Mater. 46 (2022) 452–460.
[12] J. Lopez, D.G. Mackanic, Y. Cui, Z. Bao, Nat. Rev. Mater. 4 (2019) 312–330.
[13] S. Yun, R. Xiaohui, G. Ang, et al., Nat. Commun. 13 (2022) 4181-4181.
[14] Y. Wu, Y. Li, Y. Wang, et al., J. Energy Chem. 64 (2022) 62–84.
[15] S. Bag, C. Zhou, P.J. Kim, V.G. Pol, V. Thangadurai, Energy Storage Mater. 24 (2020) 198–207.
[16] C. Liu, B. Wu, T. Liu, et al., J. Energy Chem. 89 (2024) 449–470.
[17] C. Wei, B. Xi, P. Wang, et al., Adv. Energy Sustain. Res. 4 (2023) 2300103.
[18] B. Zhao, X. Lu, Q. Wang, et al., Chin. Chem. Lett. 31 (2020) 831–835.
[19] Z. Zhang, X. Wang, X. Li, et al., Mater. Today Sustain. 21 (2023) 100316.
[20] S.P. Shen, G. Tang, H.J. Li, et al., Ceram. Int. 48 (2022) 36961–36967.
[21] Y. Li, H. Wang, Ind. Eng. Chem. Res. 60 (2021) 1494–1500.
[22] P. Shi, J. Ma, M. Liu, et al., Nat. Nanotechnol. 18 (2023) 602–610.
[23] Z. Ning, G. Li, D.L.R. Melvin, et al., Nature 618 (2023) 287–293.
[24] Y. Xiao, X. Wang, K. Yang, et al., Energy Storage Mater. 55 (2023) 773–781.
[25] L. Liu, D. Zhang, J. Zhao, et al., ACS Appl. Energy Mater. 5 (2022) 2484–2494.
[26] Y. Jiang, C. Xu, K. Xu, et al., Chem. Eng. J. 442 (2022) 136245.
[27] J.G. Ryu, R. Balasubramaniam, V. Aravindan, et al., ACS Appl. Mater. Interfaces 16 (2024) 761–771.
[28] H. Kim, J. Kim, J. Lee, et al., Energy Storage Mater. 67 (2024) 103260.
[29] X. Wang, G. Hu, Z. Peng, et al., Ionics (Kiel) 29 (2023) 3129–3142.
[30] D. Liu, Z. Lu, Z. Lin, et al., ACS Appl. Mater. Interfaces 15 (2023) 21112–21122.
[31] X. Zheng, D.Y. Xu, N. Fu, Z. Yang, J. Energy Chem. 81 (2023) 603–612.
[32] J. Zhang, S. Li, X. Wang, et al., Adv. Energy Mater. 14 (2024) 2302587.
[33] Y. Jin, Y. Li, R. Lin, et al., Small 19 (2023) 2307942.
[34] H. Noh, D. Kim, W. Lee, et al., Energies 16 (2023) 7695.
[35] Q. Lv, Y. Jing, B. Wang, et al., Energy Storage Mater. 65 (2024) 103122.
[36] F. Han, A.S. Westover, J. Yue, et al., Nat. Energy 4 (2019) 187–196.
[37] D. Jugović, D. Uskoković, J. Power Sources 190 (2009) 538–544.
[38] R. Soni, J.B. Robinson, P.R. Shearing, et al., Energy Storage Mater. 51 (2022) 97–107.
[39] C. Wang, K.R. Adair, J. Liang, et al., Adv. Funct. Mater. 29 (2019) 1900392.
[40] J. Yuan, B. Xi, P. Wang, et al., Small 18 (2022) 2203947.
[41] K. Yang, L. Chen, J. Ma, et al., Angew. Chem. Int. Ed. 60 (2021) 24668–24675.
[42] X. Ren, X. Zhang, Z. Shadike, et al., Adv. Mater. 32 (2020) 2004898.
[43] X. Ni, T. Qian, X. Liu, et al., Adv. Funct. Mater. 28 (2018) 1706513.
[44] W. Li, M. Zhang, X. Sun, et al., Nat. Commun. 15 (2024) 803.
[45] X. Han, L. Gu, Z. Sun, et al., Energy Environ. Sci. 16 (2023) 5395–5408.